Biomedical
Communication

Biosc.Biotech.Res.Comm. Vol 14 No (1) Jan-Feb-March 2021 Pp 316-327

BBRC
Bioscience Biotechnology
Research Communications

Combinational Impact of Chelerythrine and S-Allyl Cystine on *Metastasis melanoma* of liver : An *In vivo* Analysis

Sujan Chatterjee[1], Debajyoti Patra[1], Pujita Ghosh[2], Soumi Banerjee[2], Pratip Chakraborty[3], Kaustav Dutta Chowdhury[2], Anupam Basu[4] and Gobinda Chandra Sadhukhan[5*]

[1]Molecular Biology and Tissue Culture Laboratory, Post Graduate Department of Zoology, Vidyasagar College, Kolkata, India.
[2]Cyto-genetics Laboratory, Department of Zoology, Rammohan College, 102/1, Raja Rammohan Sarani, Kolkata, India.
[3]Department of Infertility, Institute of Reproductive Medicine, HB-36/A/3, Salt Lake, Sector-III, Kolkata, India.
[4]Molecular Biology and Human Genetics Laboratory, Department of Zoology, The University of Burdwan, Bardhaman, West Bengal, India.
[5]UGC-HRDC, Jadavpur University, Kolkata, India (Retd.).

ABSTRACT

Metastatic melanoma, the highly fatal and aggressive disease, has yet to any effectual remedies. Several evidences suggested delicate responsibility of oxidative/cytotoxic stress in the modulation of tumor microenvironment leading to metastasis. Therefore, conditioning of reactive oxygen species in tumour and its adjacent arena may play a guardian role for restricting metastatic melanoma. Well-known active biocomponents like S-allyl Cysteine and Chelerythrine as nontoxic dietary phytochemicals are recently documented as potential anti-tumorigenic and anti-inflammatory therapeutics but their role in metastatic melanoma still remains elusive. Therefore, present study was carried out to investigate the efficacy of S-allyl Cysteine and Chelerythrine against metastatic melanoma to the hepatic tissue. Status of liver function was estimated by performing ALT, AST, GGT and ALKP assay. ROS accumulation was determined by estimating the altered DCF fluorescence in hepatic tissue lysates. GSH and TBARS content were measured as a marker of anti-oxidant and cytotoxicity level after the treatment. Analysis on the marker proteins like Caspases, CytochromeC, BCl_2, Bax, VEGF, MMP9 and NF-κβ depicted the triggering of p-p53 nuclear translocation and significant increase in Bax expression that in-turn induced CytochromeC-Caspase9-Caspase3 apoptotic axis after drug administration. Data also illustrated notable reduction in tumor nodules at liver along-with normalization of liver function as demarcated by the level of biomarkers in the treated groups. Restoration of enzymatic and non-enzymatic anti-oxidants as well as suppression of VEGF and MMP9 expression as an effect of attenuated NFkb nuclear localization by S-allyl Cysteine and Chelerythrine effectively delimited extracellular matrix remodeling as well as angiogenesis, two major prerequisites for metastasis. Combinatorial administration of S-allyl Cysteine and Chelerythrine further portrayed better efficacy in metastatic tumor regression and tissue restoration by sustaining ROS/antioxidant balance and stabilization of p53 through its phosphorylation, that can be considered as future directives for the development of novel remedial strategy against metastatic melanoma in liver.

KEY WORDS: METASTATIC MELANOMA, ROS, ANTIOXIDANT, S-ALLYL CYSTEINE, CHELERYTHRINE.

Article Information:
*Corresponding Author: *sadhukhan.g.c@gmail.com*
Received 05/12/2020 Accepted after revision 23/03/2021
P-ISSN: 0974-6455 E-ISSN: 2321-4007
Thomson Reuters ISI Clarivate Analytics
Web of Science ESCI Indexed Journal

Identifiers & Pagination:
Vol 14(1) E-Pub 31st Mar 2021 Pp 316-327

Published by Society for Science & Nature India
DOI: http://dx.doi.org/10.21786/bbrc/14.1/45

INTRODUCTION

Melanoma, a predominant skin cancer, originates from melanocyte. Surgical removal followed by popular therapies with chemo/radiation-based drugs can cure primary melanomas. Due to its high aggressive nature and lack of complete effective therapeutic strategy, it can able to metastasize into local as well as distant organ following invasion and this in turn reduces the chances

of survivability of the patients. Therefore, majority of melanoma related morbidity is due to metastasis (Eggermont et al., 2020). Recent studies suggested that metastatic melanoma is responsible for 80% of skin cancer related fatality (Jones et al., 2020). According to the reports only 14% of malignant melanoma patients can able to survive more than 5-year (Sandru et al., 2014; Enninga et al., 2017).

Evidences from several clinical studies demonstrate distant metastasis of melanoma cells from their primary subcutaneous location (Zbytek et al., 2008 and Tan et al., 2019). Previous works also identified liver (58.3%) as the second most common target organ for metastatic melanoma (Bostanci et al., 2014; Ruini et al., 2020). Metastatic progression encompasses an array of interrelated events such as dissemination, migration and establishment of new foci, finally they then grow to develop fetal metastatic tumor silently (Palmer et al., 2011; Hao et al., 2019).

Presently many expensive therapeutic approaches like surgery followed by chemotherapy, radiation therapy and immunotherapy etc. are well practiced as remedial measures; but success rate is not significant (Sundarajan et al., 2020). Even most of them are coming up with adverse side effects (Schirrmacher et al., 2019). On this context, many phytochemicals form traditional medicine are practiced as potential anti-tumourogenic medicine considering their efficacy to suppress cancer cell proliferation by triggering apoptosis through altering the status of reactive oxygen species (ROS)- the crucial player for the sustenance of tumour microenvironment and malignant behavior of tumour cells leading to unfettered tumour progression as an effect of imbalance in pro- and anti- apoptotic proteins (Wang et al., 2012 and Kapinova et al., 2019). S-allyl Cystine (SAC) and Chelerythrine (CHEL) are two well-known naturally occurring bioactive phytochemicals with effective anti-tumourogenic effect against prostate cancer, liver cancer, breast cancer, oral cancer, neuroblastoma and non-small cell lung cancer (Kanamori et al., 2020; Yang et al., 2020).

Previous reports did not come out with any grade of subsequent toxicity in therapeutic application of those drugs in *in vivo* cancer treatment of nude mice model (Chmura et al., 2000 and Ng et al., 2012). SAC is an aged garlic derived water soluble, stable organo-sulfur compound. Studies suggested the ability of SAC in the suppression of cell growth, cell proliferation, metastasis and induction of apoptosis by modulating cellular ROS dependent activities (Shang et al., 2019). CHEL is a benzo-phenanthridine alkaloid commonly isolated from herbal plants like *Cheludonium majus, Macleaya cordata* and *Sanguinaria canadensis* (Kumar et al., 2013). Various reports suggested anti-diabetic, anti-microbial, anti-inflammatory, anti-fungal and even anti-cancerous properties of CHEL (He et al., 2018).

Previous reports also exhibited CHEL mediated apoptosis in prostate and renal cancer cells through activating ROS mediated intrinsic cell death pathway (Wu et al., 2018; He et al., 2020). SAC was also able to inhibit the proliferation of melanoma cell lines in a dose-dependent manner and demonstrated significant cytotoxic effects on Sk-mel3 melanoma cell line as observed in *in vitro* assay (Hakimzadeh et al., 2010). Reports demonstrated the provoking role of CHEL in the development of apoptotic response in uveal melanoma cells (Kemeny-Beke et al., 2006).

Moreover, potential role of CHEL in the suppression of proliferation and metastasis of human prostate cancer cells via modulating MMP/TIMP/NF-κB system as well as inhibition of the migration and invasion of Hep3B cells in a dose-dependent manner along with change of cell structure were reported (Yang et al., 2020). While a series of *in vitro* experiments including MTT, colony-forming, wound-healing, invasion, apoptosis and cell cycle assays demonstrated anti-proliferative and anti-metastatic effects of SAC on the metastatic HCC cell line MHCC97L (Ng et al., 2012).

SAC treatment also significantly reduced the migration of A2780 cells, and markedly decreased the expression of key proteins such as Wnt5a, p-AKT and c-Jun, involved in proliferation and metastasis (Xu et al., 2014). Observations indicated that oral administration of SAC not only inhibited the growth of primary tumors but also reduced the occurrence of lung and adrenal metastases by without causing notable toxicity. This metastatic suppression was accompanied by a distinct reduction of viable circulating tumor cells, supporting the potential use of SAC as an E-cadherin up-regulating antimetastatic agent for the treatment of androgen-independent prostate cancer (Kanamori et al., 2020).

Although, therapeutic efficacy of SAC and CHEL on metastatic melanoma, categorically in liver, still remains elusive. Here, in this study, we aimed to investigate therapeutic effect of SAC and CHEL, individual as well as in combination, on the ectopic metastatic mice melanoma tumor model. Experimental results depicted that SAC and CHEL administration-maintained ROS/antioxidant balance and stabilized p53-axis through its phosphorylation resulting significant increase in Bax expression that in-turn turned on intrinsic apoptotic pathway.

Data also first time illustrated the reduction in tumor nodules at liver and normalization of liver function in the treated groups. Analysis on related molecular status suggested effective delimitation of extracellular matrix remodeling and angiogenesis by SAC and CHEL via suppressing VEGF and MMP9 expression as an effect of reduced level of NFκ translocation towards nucleus. Hence in the summary, our findings first time described the novel therapeutic role of SAC and CHEL against B16F10 induced metastatic melanoma in *in vivo* and their potential anti-metastatic properties need to be scrutinized in other *in vivo* and clinical studies on urgent basis to give a probable ray of hope in the designing of therapeutics against metastatic melanoma in future.

MATERIAL AND METHODS

Unless and until mentioned all chemicals and reagents were purchased from Merck-Millipore, USA. B16-F10, a well-established murine mice melanoma cell line, were collected from IICB, Kolkata, originally purchased from ATCC, Manassas, Virginia and cultured in Dulbecco's modified Eagles medium (HiMedia, Mumbai, India) supplemented with 10% fetal bovine serum (HiMedia, Mumbai, India), 1% PenStrep (Life BioSciences, USA) and 0.1% Fungizone (Life BioSciences, USA) at 37 ^{0}C and 5% CO2 containing humidified air (Chowdhury et al., 2019 B). Five-week aged male Balb/C mice of 12-15gm weight were purchased and housed in micro-isolator cages with 12h day/night cycle under hygienic condition. Animal house was maintained at 27$\pm$3^{0}C with a relative humidity of 50-62%. Mice were free access of standard pellets as food and water through *ad libitum*. All animal experiments were designed following Institutional Animal Ethical Committee Guidelines to reduce the animal sufferings without hampering the requisites of statistical analysis (Sengupta et al., 2017 A).

B16F10 melanoma cells were injected subcutaneously to the left thigh at a dose of 2X10^6 cells in 200µl phosphate buffered saline (PBS). Primary tumour was first visualized after 5-6 days of cell inoculation and progression was noticed day by day. This group was labelled as ST. Only PBS injected control animals were simultaneously maintained as a separate group (n=5) with same diet and were tagged as Con. After five weeks of B16F10 cell exposure, a group (n=5) of ST animals were treated daily with individual SAC (ST+SAC) and CHEL (ST+CHEL) at a dose of 250mg/kg b.w. and 5mg/kg b.w., respectively, through gavage for 30days and 60days, sequentially. Again, another ST group of animals (n=5) received daily 250mg/kg b.w. SAC in combination with 5mg/kg b.w.

CHEL through gavage for 30days, 45days and 60days and were denoted as ST+SAC+CHEL. Three separate groups (n=5) of Con mice were treated with 250mg/kg b.w. SAC, 5mg/kg b.w. CHEL and 250mg/kg b.w. SAC+5mg/kg b.w. CHEL for 60days as negative control and were marked as Con+SAC, Con+CHEL, Con+SAC+CHEL, respectively (Kumar et al., 2015; Chatterjee et al., 2019). Alterations in morphology were identified as dark patches of melanin synthesis and were evaluated by calculating tumour numbers in total ten quadrates (Bostanci et al., 2014). Number of tumour nodules was represented in 4x4mm2 area. Blood was collected from treated as well as untreated control, B16F10 infused, individual and combined drug treated animals and serum was isolated according to the standard protocol (Chatterjee et al., 2019).

Prepared serum was used as protein source for evaluating the activities of aspartate transaminase (AST), alkaline phosphatase (ALKP), alanine transaminase (ALT) and γ-glutamyl transferase (GGT). Assays were performed by following respective manufacturing kit protocols at room temperature. ALT and AST (TECO Diagnostics, CA, USA) activity was measured by estimating NADH oxidation at 320nm of wavelength for 30s intervals up to 2min. ALKP and GGT analysis absorbances were measured at 405nm for 30s intervals. Results were evaluated by determining mean absorbance change per minute. Values were portrayed in IU/L (Chatterjee et al., 2019). To evaluate TBA reactive substrate (TBARS) content, liver tissue was lysed in 10mM TRIS-HCl lysis buffer pH 7.4 and was used for experimental analysis. 0.4mg of protein in 100µl lysis buffer was added with 2ml TBA-TCA and was boiled for 20min at 100 ^{0}C water bath. Solution was centrifuged at 1000g for 10min at room temperature and absorbance of supernatant was measured at 532nm. Values were represented as nmol/mg protein (molar extinction coefficient: 1.56x105 M^{-1} cm^{-1}) (Chatterjee et al., 2019).

Hepatic tissue samples were deproteinized with 35% metaphosphoric acid (Ref). Extracted samples were neutralized with 0.3M Na2HPO4. 0.6mM DTNB, 0.5U GR and 0.2mM NADPH were added as final concentration to the reaction mixture. Formation of reduced glutathione-DTNB conjugate within supernatant was then measured spectrophotometrically at 412nm (Sengupta et al., 2017 A). Data were presented in mole/mg protein. Superoxide dismutase (SOD) activity was measured from chloroform methanol extract following the standard protocol (Sengupta et al., 2014).

Values were quantified spectrophotometrically (UV-1240 Pharma Spec, Shimadzu, Kyoto, Japan) by calculating the changes in pyrogallol auto-oxidation at 420nm in presence of catalase enzyme. One unit of SOD activity is equal to the 50% suppression of superoxide mediated oxidation of pyrogallol. Results were represented in unit/mg protein. Catalase activity was evaluated through spectrophotometrically (UV-1240 Pharma Spec, Shimadzu, Kyoto, Japan) by measuring degradation of H2O2 in presence of tissue lysate as a source of enzyme. Values were quantified by measuring absorbances at 240nm in 10s intervals. Data were represented in unit/mg protein (Sengupta et al., 2017 A).

Cells of the liver were isolated from experimental groups by Collagenase-IV digestion. Intracellular ROS was measured by incubating 5% cell suspension with 5µM 2,7-dichlorofluorescein diacetate (DCFDA) (Sigma-Aldrich, St. Louis, Missouri, USA), a fluorogenic dye, at 37 ^{0}C for 15min. After diffusion it was deacetylated by cellular esterase to a non-fluorescent compound which was later oxidized by ROS into highly fluorescent 2,7-dichloroflurescin (DCF). Emitted fluorescence (Ex: 485nm/ Em: 535nm) was estimated in RF-6000 Fluorescence Spectro-fluorometer (Shimadzu, Kyoto, Japan). Values were presented in Relative Fluorescence Unit (RFU) (Sengupta et al., 2014).

Liver tissue of experimental groups was lysed by lysis buffer following kit (Bio Vision, USA) protocol and was used as protein source for Caspase3 as well as Caspase9 activity assay (Sengupta et al., 2017 A). 100µg of protein in 50µl lysis buffer was loaded in Caspase3p17 antibody (capture antibody) coated microtiter plate, for Caspase3

analysis and in cleaved-Caspase9p37 antibody (capture antibody) coated microtiter plate, for Caspase9 analysis. After 4h incubation at 4^0C 5µl 4mM DEVD-pNA was added as substrate solution and was again incubated at 37 ^{0}C for 2h. Activities of Caspase3 and Caspase9 were evaluated by measuring the released pNA absorbance at 405nm and were represented in pmol pNA/min/mg protein (Chatterjee et al., 2019; Chao et al., 2019).

Bcl2, Bax, CytochromeC, phospho-p53/Ser15, NFκβ/p65, VEGF and MMP9 were quantified by using commercially available specific Elisa kit (R&D Systems Inc. Minneapolis, USA) following respective manufacturer instruction. Cytosolic fractions were prepared according to the standard kit protocol (Nuclear/Cytosol fractionation kit, K266, Cell Biolabs) and were used as protein source for quantitative analysis of cellular Bcl2, Bax, CytochromeC, VEGF and MMP9. While nuclear fractions were prepared following standard kit protocol (Nuclear/Cytosol fractionation kit, K266, Cell Biolabs) and were similarly used for the estimation of nuclear NFκβ/p65 and phospho-p53/Ser15 content (Li et al., 2018). Values were measured at 450nm and were calculated through provided standard curve. Results were represented in ng/ml protein. Data were mean±SD. Differences between treated and untreated groups were evaluated by student's t test in GraphPad Prism software, La Jolla, CA, USA. P≤0.05 was considered as statistically significant.

RESULTS AND DISCUSSION

Model development, morphometric and survivability analysis: Herbal medicine is a potent remedial measure against neoplastic liver (Li et al., 2011; Yang et al., 2020). Previously, some *in vitro* analysis documented anti-metastatic effect of SAC against, prostate cancer, neuroblastoma, hepatocellular carcinoma and ovarian cancer, but not in the field of metastatic melanoma. Remedial efficacy of SAC against primary melanoma cell lines was previously described by researchers, and noted as a potent restricting player for the melanoma cell proliferation in *in vitro* system (Hakimzadeh et al., 2010; Xu et al., 2014). Similarly, researchers established the therapeutic advantage of CHEL administration against dalton's lymphoma, liver cancer, breast cancer and renal cancer in both *in vitro* and *in vivo* condition (Kumar eta al., 2015).

According to the reports benefit of CHEL administration was studied on OCM-1, the well-known melanoma cell line (Chen et al., 2016). Data suggested the discrete role of the treatment in DNA fragmentation as well as apoptosis induction of this primary cancer cells. Thus, previous reports pointed out the efficacy of individual administration of SAC and CHEL in the attenuation of tumor progression and healing of several primary cancers like prostate, liver, colorectal, lung and skin but their impacts on metastasis to distant organs (*in vivo* studies) specially in melanoma still remain unknown (Xu et al., 2014).

Moreover, no previous reports were found about the importance of combined treatment in this regard. Therefore, to deduce the therapeutic efficacy of SAC and CHEL against metastatic melanoma, spontaneous metastatic animal model was developed by injecting 2X106 B16F10, the perpetual melanoma cell line, at left thigh region of Balb/c mice (Bostanci et al., 2014). Nascent primary tumor was visualized after 5/6 days of cell inoculation at the mentioned site. Also, sharp and gradual increase in primary tumor volume was detected. Secondary tumor was first noted at liver after 21 days of cell inoculation. Unusual dark patches, due to accumulation of melanin within melanoma cells, was visualized and was considered as secondary growth of subcutaneous melanoma at liver. Nodule numbers were increased along with the increase in days and 7-9 metastatic nodules were noted per 4X4 mm2 of liver (Fig.1A) (ST) after 35 days of inoculation. 250mg/kg b.w. SAC (ST+SAC) and 5mg/kg b.w. CHEL (ST+CHEL) significantly regressed tumor number after 30 and 60 days of post treatment; while remedial efficacy was increased effectively in SAC+CHEL combinatorial approach ($p<0.01$).

Figure 1: SAC and Chelerythrine treatment restored liver morphology and function in B16F10 melanoma cell induced metastatic tumor bearing mice
Number of nodules at liver collected from control, B16F10 cell injected and individual 250mg/kg b.w. SAC, 5mg/kg b.w. CHEL as well as 250mg/kg b.w. SAC+ 5mg/kg b.w. CHEL co-treated groups of mice, were estimated and represented in average number of nodules/4X4mm2 (A). Survivability analysis (B) was measured and represented in number of survival animals. Liver stress specific bio markers ALT (C), ALKP (D), GGT (E) and AST (F) were estimated in blood serum isolated from untreated and treated control, B16F10 cell injected and individual 250mg/kg b.w. SAC, 5mg/kg b.w. CHEL as well as 250mg/kg b.w. SAC+ 5mg/kg b.w. CHEL co-treated groups of mice. Values were represented in IU/L. Data were expressed as mean±SD and were obtained from six independent experiments (n=5). NS,*p<0.01 vs Control, #p<0.01 vs ST. Con=Control, SAC=S-allyl Cystine, CHEL= Chelerythrine, ST= Secondary Tumor.

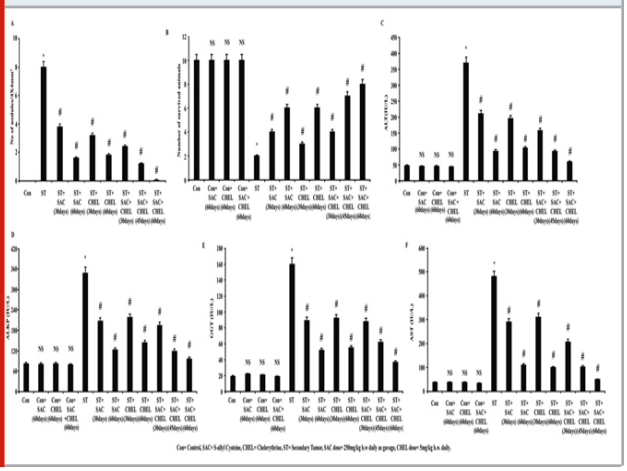

Following 45days of 250mg/kg b.w. SAC treatment in combination with 5mg/kg b.w. CHEL (ST+SAC+CHEL) reduced number of tumor nodules effectively than 60days individual drug treatment ($p<0.01$). Results also depicted more or less elimination of all metastatic melanoma nodules as well as that eventually restored hepatic morphology ($p<$NS vs. Control) (Fig. 1A) more or less similar to control mice after 60days of combined treatment. Comparative drug trials use risk of survival analysis during the assessment of clinical efficacy (Dahal et al., 2019). Considering this technical perspective experiments were designed and values from survivability analysis depicted a sharp decrease in numbers of survived animals in B16F10 inoculated ST groups after 95days of experimental schedule.

One month treatment with either of the single drug (ST+SAC/ST+CHEL) and in combination (ST+SAC+CHEL) demonstrated considerable increase in survivability rate ($p<0.01$). Combined therapy (ST+SAC+CHEL) for 45days and especially for 60days depicted distinct reduction in mortality rate than 60days of individual drug treated groups ($p<0.01$) (Fig.1B). Non-significant alterations in survivability rate (Fig.1B) were noticed in individual and combinatorial treatment for 60days in control group of mice.

Estimation of biochemical stress markers specific for liver function after S-allyl Cystine and Chelerythrine treatment in B16F10 induced metastatic melanoma at liver: Alanine aminotransferase (ALT), alkaline phosphatase (ALKP), γ-glutamyl transferase (GGT) and aspartate aminotransferase (AST) activity in plasma are well-known serum biomarkers for the estimation of liver injury and function (Lala et al., 2020). Altered activities of those stress specific biomarkers are the indicative of abnormalities in liver homeostasis. Data illustrated significant increase in plasma ALT, AST, ALKP and GGT level in ST groups. Values also depicted a trend of gradual regression of all the biomarkers after individual SAC or CHEL treatment (ST+SAC/ST+CHEL) for 30days and 60days.

Analysis suggested that ALT, AST, ALKP and GGT activities ($p<0.01$) after 45days of co-treatment with SAC+CHEL (ST+SAC+CHEL) were in a range of individual SAC or CHEL treatment for 60days. Whereas most significant efficacy ($p<0.01$) was noticed after 60days of combined (ST+SAC+CHEL) therapy (ALT=58.7892$\pm$5 IU/L, AST= 48.7892$\pm$5 IU/L, ALKP=79.7892$\pm$5 IU/L, GGT=36.7892$\pm$5 IU/L) ($p<0.01$). No considerable alterations were documented in either of ALT, AST, AKLP and GGT levels in individual or combined treatment for 60days in control mice (Fig.1C, 1D, 1E, 1F) indicating no such effectual toxic impact of the said drugs both in individual and combined schedule.

During metastasis migratory tumor cells invade into distal location and establish tumorigenic growth (Fares eta l., 2020). In the present study aggressive melanoma cell B16F10 demonstrated metastatic migration and colonization, proliferation and finally development of secondary tumors in the liver. Our data suggested that incidence of metastatic melanoma hampers normal liver function and physiological activity as observed other fatal liver injuries (McGill et al., 2019).

Disease severity as well as liver injury was gradually progressed with the increase in nodule numbers similar to the previous observations on liver cancer (Simoes Eugenio et al., 2020). Various contemporary researchers already portrayed SAC and CHEL as an effective drug against hepato-cellular carcinoma, liver cirrhosis and other liver diseases (Chmura et al., 2000; Ng et al., 2012). In our study, results first time noted noteworthy improvement of animal survivability by restoring liver morphology and homeostasis in B16F10 infused mice after SAC and CHEL combined treatment. Hence, combinatorial practice can able to heal metastatic melanoma at liver and this finding pointed us to look over the underlying aspects behind this remedial effect.

Evaluation of tissue specific stress and associated factors in B16F10 infused mice: According to the reports, SAC and CHEL are potential free radical scavengers and are able to modulate various ROS dependent biological activities like: cell survivability, cell proliferation, metabolic activity, apoptosis, etc. (Chen et al., 2016; Sengupta et al., 2017). Serum markers are also modified by the interactions of ROS with the antioxidant system present in the tissue microenvironment (Sengupta et al., 2017). Here elevated levels of liver stress specific biomarkers instigated us to study about the enzymatic as well as non-enzymatic anti-antioxidants and accumulation of the oxidized products/ reactive oxygen species since the imbalance between ROS and anti-oxidants, similar to previous studies, might be responsible for the development of liver stress in our study.

Analysis of enzymatic antioxidant pool was performed by measuring SOD and Catalase activity in liver isolated from control, ST and SAC/CHEL treated as well as co-treated (ST+SAC+CHEL) groups of animals. Results depicted reduced SOD (16.89234 Unit/mg protein) and very low catalase (5.8990234 Unit/mg protein) activities in liver of ST group of mice; although SOD and Catalase activities were repleted along the course of SAC and CHEL treatment for 30 and 60days. 45days of co-treatment demonstrated the values in a range of 60days of individual treatment while most effective repletion was noticed after 60days of co-treatment (ST+SAC+CHEL) ($p<0.01$) (Fig. 2A, 2B). Non-enzymatic antioxidant assay comprises of reduced glutathione (GSH) analysis.

Data suggested reclaiming of GSH content after both 30 as well as 60days of individual treatment and co-treatment category portrayed similar improvement as before specially after the schedule of 60days (Fig. 2C). No considerable changes were revealed in SOD (Fig. 2A), Catalase (Fig. 2B) activities and GSH level (Fig. 2C) after 60days of individual or co-treatment of control mice. Thiobarbituric acid reactive substance (TBARS) content was estimated as an indication of cytotoxic stress (Chatterjee et al., 2019). Data indicated notable

enhancement of TBARS in liver collected from ST mice (7.79203405 nmol/mg protein) and value was normalized after individual and co-treatment with SAC and CHEL.

Observation further indicated the most significant reduction only after 60days of co-treatment (ST+SAC+CHEL) (1.892345 nmol/mg protein) ($p<0.01$) (Fig. 2D). Direct estimation of ROS was performed using DCFDA as fluorescent probe. Analysis depicted a noteworthy enhancement of DCF fluorescence in liver collected from ST group ($p<0.01$) with a trend towards normalization of cellular ROS in the treated groups. Values illustrated effective suppression of ROS in co-treated (ST+SAC+CHEL) group after 45 days and highest level of reduction was noticed after 60days ($p<0.01$) of treatment. No significant alteration was noted in DCF fluorescence and TBARS content after 60days of individual or combined treatment of control mice (Fig.2E).

Figure 2: Estimation of alteration in reactive oxygen species, TBARS content and antioxidant system after SAC and Chelerythrine administration

Lysates were processed from liver of untreated and treated control, B16F10 cell injected and individual 250mg/kg b.w. SAC, 5mg/kg b.w. CHEL as well as 250mg/kg b.w. SAC+ 5mg/kg b.w. CHEL co-treated mice. Status of enzymatic antioxidant level was estimated through measuring SOD (A) and catalase (B) activities and was represented as Unit/ mg protein. GSH (C) and TBARS (D) content were measured and were represented as nmol/mg protein. Level of reactive oxygen species was estimated by measuring DCF fluorescence (E) and was represented in RFU. Values were expressed as mean ±SD and were obtained from six independent experiments (n=5). NS,*p<0.01 vs Control, #p<0.01 vs ST. Con=Control, SAC=S-allyl Cystine, CHEL= Chelerythrine, ST= Secondary Tumor.

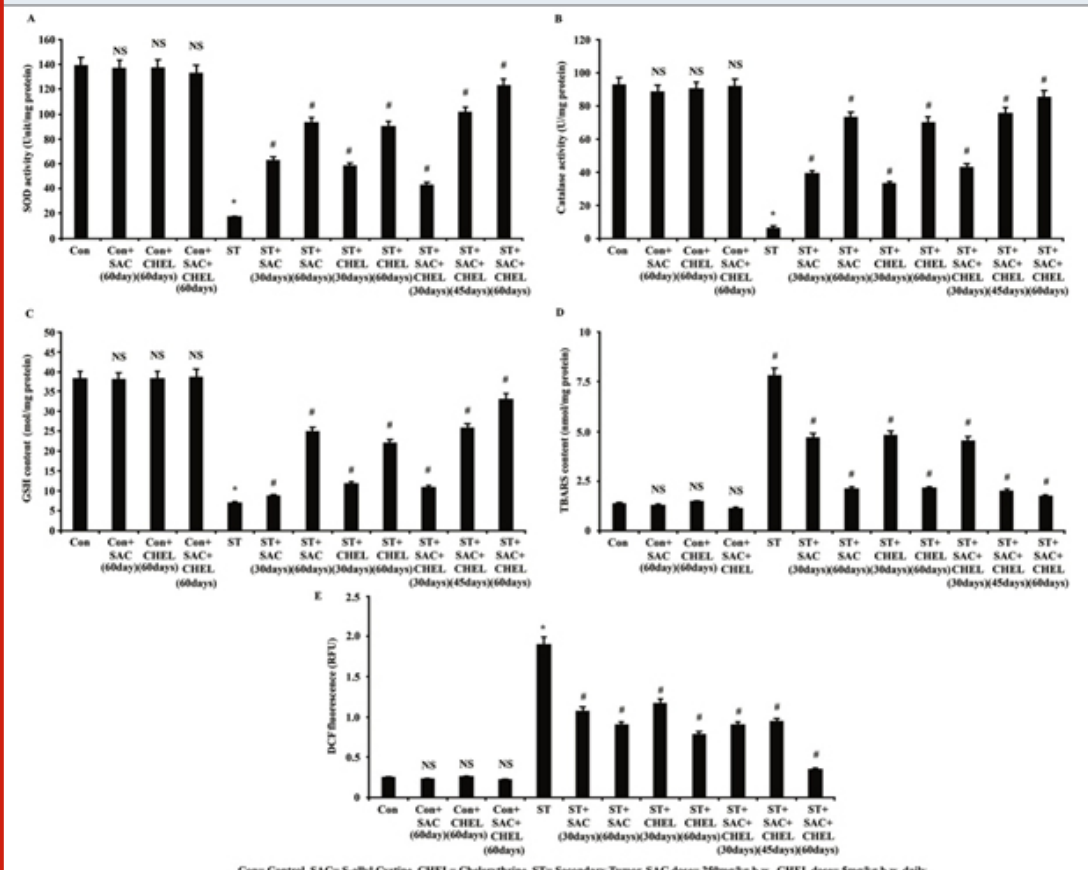

According to the reports ROS is generated in the form of highly reactive free radical superoxide which is dismutated into oxygen and hydrogen peroxide through enzymatic activity of SOD (Sengupta et al., 2017 A). Catalase further scavenges H2O2 to convert it into water and O2; in this way accumulation of ROS is averted (Sengupta et al., 2017 A). According to the present study tumour site of the liver in secondary melanoma showed very poor SOD and catalase activity along with a significant suppression of GSH content that probably nourished tumor microenvironment and helped in metastatic tumor formation.

SAC and CHEL treatment effectively augmented both enzymatic as well as non-enzymatic antioxidant system and accumulated ROS was neutralized by elevated catalase activity, finally hydrolyzed to non-toxic substance water and oxygen. Increase in GSH content

also added further protection to the tissue from oxidative stress. By scavenging ROS these anti-oxidant drugs also suppressed TBARS content similar to the effects as noted in other carcinogenic studies (Sang et al., 2019). This in turn probably helped to restrict metastatic tumor progression. So, the study experimentally proved the tuning role of SAC and CHEL in the maintenance of a balance between anti-oxidants and accumulated ROS leading to modulation of hepatic physiology as reflected in biomarker analysis, most significantly in combined approach (Sang et al., 2019).

Assessment of growth associated regulatory factors in B16F10 induced metastatic melanoma at liver: Cancer cell proliferation and tumour establishment are associated with negative modulation of the apoptosis (Connor et al., 2019). Reports suggested significant association of ROS with the regulation of apoptosis in cancer cells (Sang et al., 2019). Researchers further demonstrated the impacts of ROS in the reduction of growth of various primary tumors originated at colon, breast, liver, lung etc. in both *in vivo* and *in vitro* condition (Sengupta et al. 2017). Previous studies recommended chief executive role of caspases in the conduction of apoptosis (Phillips et al., 2020).

Considering the instructive responsibility of ROS in guide lining the Caspases here activities of Caspase9 as initiator and Caspase3 as executioner were studied for mechanistic analysis (Li et al., 2020). Results depicted significant enhancement in the activity of both Caspase9 (Fig. 3B) and Caspase3 (Fig. 3A) ($p<0.01$) in the liver of ST group of mice after individual as well as combined SAC and CHEL treatment. Interestingly activities of the Caspases were increased after 45days of combined therapeutics against individual treatment of either of the drugs ($p<0.01$); while continuation of the treatment up to 60days revealed distinct reduction in activities of both of the enzymes towards the level of control animal (Fig. 3A, 3B).

Figure 3: Evaluation of changes in CytochromeC distribution-caspase activity after SAC and Chelerythrine treatment

Estimation of Caspase3 (A) and Caspase9 (B) activity in whole cell lysate of liver isolated from untreated and treated control, B16F10 infused and individual 250mg/kg b.w. SAC, 5mg/kg b.w. CHEL as well as 250mg/kg b.w. SAC+ 5mg/kg b.w. CHEL co-treated group; were represented in pmol pNA/min/ mg protein. Cytoplasmic CytochromeC level (C) in cytoplasmic fraction of the above-mentioned lysates was quantified and were represented in Unit/mg protein. Data were mean±SD and were obtained from six independent experiments (n=5). NS,*$p<0.01$ vs Control, #$p<0.01$ vs ST. Comparative analysis in-between Caspase3, Caspase9 activity with released CytochromeC was portrayed in figure 3D. Values were mean±SD and were obtained from six independent experiments (n=5). Con=Control, SAC=S-allyl Cystine, CHEL= Chelerythrine, ST= Secondary Tumor.

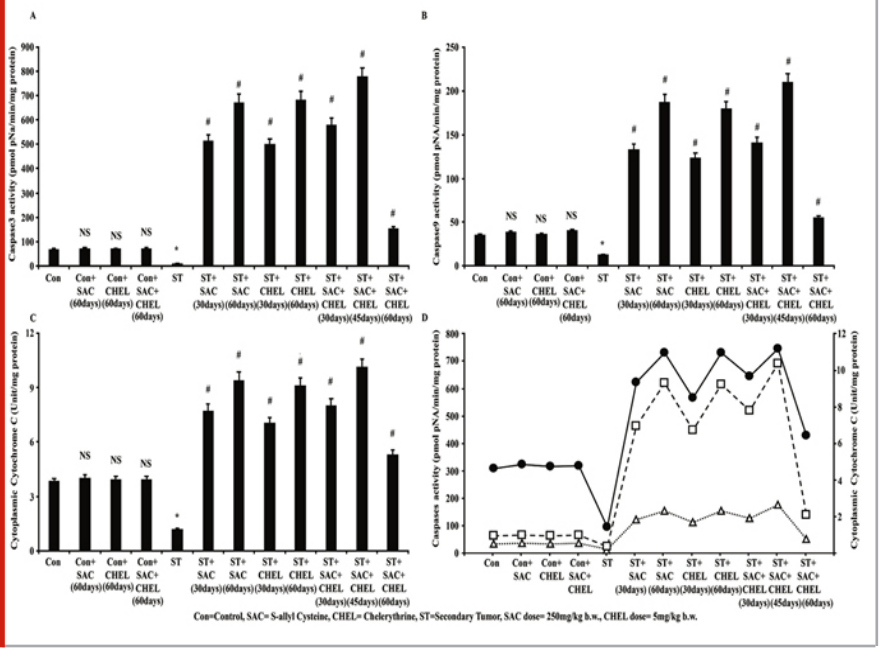

Caspase9 activity is dependent upon the release of mitochondrial CytochromeC to the cytoplasm which is again dependent upon accumulation of intracellular ROS as suggested (Li et al., 2020). Data demonstrated significant increase in CytochromeC content in cytoplasmic fraction of liver isolated from individual

and with a peak in 45days of combined drug treated group ($p<0.01$). Although similar to Caspase9 activity of CytochromeC was markedly reduced towards control level after 60days of combined treatment (Fig 3C). No such noteworthy changes were visualized in Caspase3 (Fig. 3A), Caspase9 (Fig. 3B) activities and cytoplasmic CytochromeC distribution (Fig. 3C) after 60days of individual or combined treatment to control mice (Lin et al., 2020).

Combined ray diagram of CytochromeC level in cytoplasm with the activities of both of the Caspases portrayed similar trend in the changes following the scheduled treatment suggesting a potential role of cytosolic CytochromeC in the activation of Caspases in metastatic melanoma tumor containing area of liver of B16F10 infused mice (Fig 3D). It is well evident that Cytochrome C- Caspase axis is turned off in cancer cells that in turn helped in tumor progression and metastasis. In our study SAC and CHEL administration effectively tuned on ROS dependent CytochromeC-Caspase axis and significantly induced apoptosis in colonized metastatic melanoma cells at liver. Similar effects were reported in the primary cancers like colorectal cancers, liver cancer and breast cancer (Chen et al., 2016 and Sengupta et al. 2017). Therefore, the proposed therapeutics significantly reduced symptomatic impacts in the B16F10 infused mice by triggering caspase mediated cell death at secondarily developed melanoma in liver as observed in our study.

Estimation of the status of biomolecules responsible for SAC and CHEL induced apoptosis, tissue degradation and angiogenesis: According to the previous reports cytoplasmic level of CytochromeC is significantly lower in the colony of cancer cells (Yau et al., 2019). Release of CytochromeC into cytoplasm is harmonized by proapoptotic-antiapoptotic balance and generally increased level of cytoplasmic CytochromeC level indicates an imbalance between Bax and Bcl2, the well-known proapoptotic and antiapoptotic proteins, respectively (Sengupta et al. 2017).

Figure 4: Estimation of the status of apoptotic, angiopoietic and ECM degrading guardian factors after SAC and Chelerythrine treatment
Bcl2 (B), Bax (C), VEGF (D), MMP9 (E) expression were measured in whole cell lysate and level of phopho-p53-Ser15 (A) and NFκβ/p65 (F) were estimated from nuclear fraction of the liver isolated from untreated and treated control, B16F10 cell injected and individual 250mg/kg b.w. SAC, 5mg/kg b.w. CHEL as well as 250mg/kg b.w. SAC+ 5mg/kg b.w. CHEL co-treated group; were represented in ng/ml protein. Results were mean±SD and were obtained from six independent experiments (n=5). NS,*$p<0.01$ vs Control, #$p<0.01$ vs ST. Comparative analysis of phopho-p53-Ser15, Bcl2, Bax, VEGF, MMP9 and NFκβ/p65 levels among control, B16F10 cell injected and individual 250mg/kg b.w. SAC, 5mg/kg b.w. CHEL as well as 250mg/kg b.w. SAC+ 5mg/kg b.w. CHEL co-treated groups and was represented in spider chart (G). Con=Control, SAC=S-allyl Cystine, CHEL= Chelerythrine, ST= Secondary Tumor.

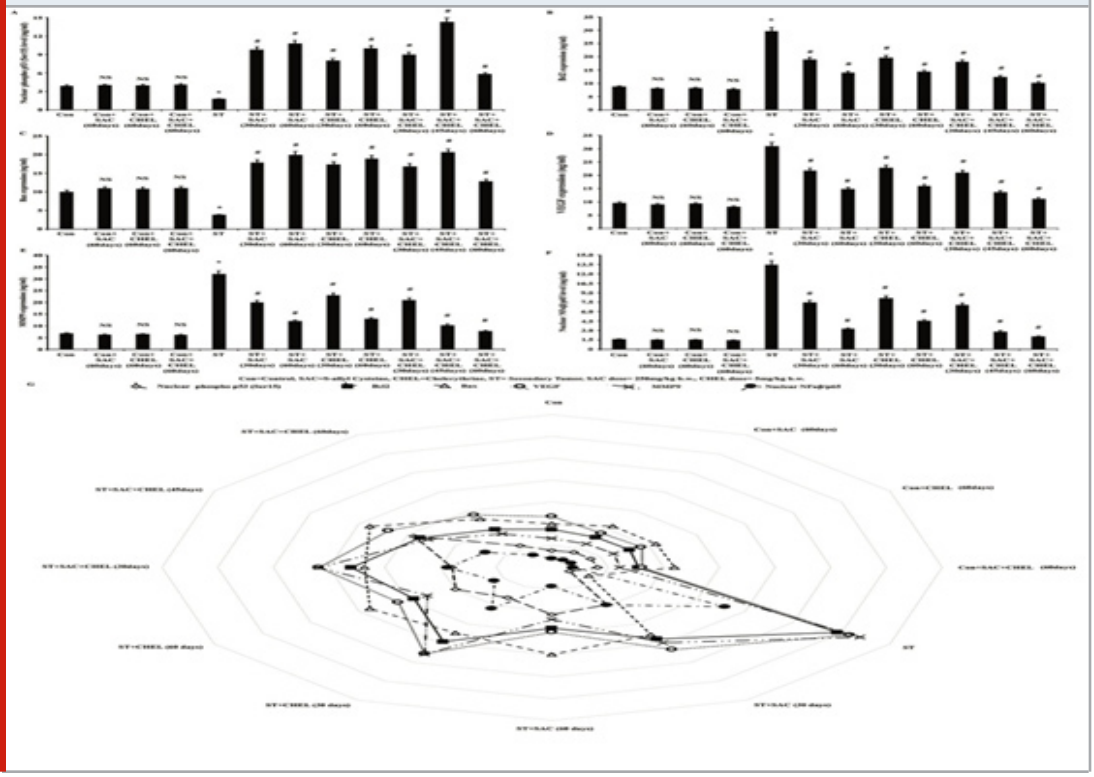

Various studies also suggested the imperative role of stabilized p53 in the up-regulation of Bax expression leading to CytochromeC release into cytoplasm from mitochondria (Somade et al., 2020). Recent reports further suggest the wobbly level of p53 in the colonized cancer cells (Capaci et al., 2020). Present analysis demonstrated the elevated level of Bax in cytoplasm (Fig. 4C) and phospho p53-Ser15 in nuclear fraction (Fig. 4A), the stabilized from of p53 and a potential transcriptional factor of Bax, in both individual SAC and CHEL as well as 45days of combined treatment of ST animals ($p<0.01$). Further continuation of the combined treatment for another 15days showed a downfall of Bax (Fig. 4C) and phospho p53-Ser15 (Fig. 4A) level towards control animal.

While Bcl2 expression was significantly decreased along the course of the schedule both in individual and combined treatment and value after 60days of SAC+CHEL treatment demonstrated a range nearing to control mice ($p<0.01$) (Fig. 4B). No significant change was revealed after 60days of individual or combined treatment to control group of mice ($p<0.01$) (Fig. 4A, 4B, 4C). Therefore, SAC and CHEL treatment appreciably induced p53-Bax axis which was responsible for the activation of Cytochrome C-caspase pathway as observed in our study and probably took a part in controlling the melanoma cell progression in the liver as secondary site. Angiogenesis and modification in extracellular matrix by the factors secreted from cancer cells alter tumor microenvironment and help in metastatic invasion (Fares et al., 2020). It is evident that ROS can able to increase angiogenic processes and ECM remodeling via uplifting the expression of assisting factors like matrix metalloproteinases (MMPs) in the carcinogenic foci of a tissue (Bockmann et al., 2020).

Recent studies mentioned that attenuation of angiogenic regulatory (Ang-I, Ang-II, VEGF, etc.) and extracellular matrix degrading (MMP-2, MMP-3, MMP9, etc.) factors perform the crucial job related to the suppression of metastasis and reduction of tumor volume in liver, colorectal and prostate carcinoma as well as retinoblastoma, etc. (Chan et al., 2020). Result illustrated reduction of VEGF ($p<0.01$) (Fig. 4D), a well evident prime nourishing protein for angiogenesis and MMP9 ($p<0.01$) (Fig. 4E), factor that helps in the progression of metastatic tumor through restructuring extracellular matrix expression after individual SAC or CHEL as well as combined treatment categorically after 60days of SAC+CHEL treatment to ST group of mice (Fig. 4D, 4E). No effective alterations were suggested after individual and combined treatment to control animal (Fig. 4D, 4E).

Our studies further demonstrated significant nuclear localization of NFκβ/p65 in the metastatic site of the liver in B16F10 infused mice. According to the reports nuclear translocalization of NFκβ/p65 trigger VEGF and MMP9 expression to the tumorigenic site in parallel to ROS accumulation that in turn generates a a microenvironment favorable to further invasion and sustenance of the metastasis (Viswnadha et al., 2020). Nexus between the ROS and NFκβ/p65 nuclear localization along with VEGF and MMP9 expression guided us to investigate the status of NFκβ/p65 after SAC and CHEL treatment in our experimental model.

Present study evidently portrayed effective repression in nuclear localization of NFκβ/p65 both after individual as well as combined treatment with a most significant reduction after 60days of SAC+CHEL treatment and the value was nearly the level of control animal ($p<0.01$) (Fig. 4F). No such distinct alterations in NFκβ/p65 nuclear localization were noted after 60days of individual and combined treatment of control mice (Fig. 4F). Data presentation in spider chart of phospho p53-Ser15 and NFκβ/p65 level within nucleus, Bcl2, Bax, VEGF and MMP9 expression demonstrated their association with the alterations in liver of ST group of mice.

In summary categorical reduction in phospho p53-Ser15 nuclear localization and Bax expression as well as corresponding augmented Bcl2 expression in parallel to enhancement in NFκβ/p65 nuclear localization leading to increase in VEGF and MMP9 expression helped in development of a microenvironment favourable for the establishment of secondary melanoma in the liver of B16F10 infused mice. Analysis suggested increase in phospho p53-Ser15 nuclear localization-Bax expression, reduced Bcl2 expression, reduction in NFκβ/p65 nuclear localization, VEGF as well as MMP9 expression in individual and distinctly after 45days of combined treatment. Cumulatively the said scenario was probably responsible for the reduction of the tumorigenic growth at the metastatic sites of the liver in our model.

Moreover, 60days of SAC+CHEL treatment demonstrated a range of all parametric values tending towards control mice. Values indicated probable restoration of the tissue along with significant reduction of morphological alterations of the liver developed due to metastatic melanoma in ST group of mice (Fig. 4G). In the end it can be stated that our *in vivo* study was first time designed to evaluate anti metastatic property of individual as well as combined therapeutic effect of SAC and CHEL against metastatic melanoma in liver. The results clearly stated the efficacy of this therapeutic approach in the suppression of metastatic melanoma and normalization of native liver physiology.

Better efficacy in switching on the p53- Bax-CytochromeC axis along with reduction in NFκβ/p65 dependent VEGF and MMP9 expression after 45days of SAC+ CHEL administration pointed out the importance of combined therapy. Way of normalization of the mentioned apoptotic signaling as well as VEGF/MMP9 level with the sustained antioxidant balance after 60days of SAC+CHEL treatment indicated effectual restoration as also suggested by the liver specific biomarker assay (Viswnadha et al., 2020).

CONCLUSION

In summary, our work confirmed the role of SAC and

CHEL as effective anti-metastatic agents that were able to target p53, as well as NFκβ dependent signaling orchestras and cured metastatic melanoma at liver by calibrating tissue ROS/anti-oxidant malady. Data further asserted improved remedial efficacy along-with no such toxicity effects in combined therapeutics. Therefore, SAC and CHEL administration in combination may be considered for formulating effectual therapeutics to treat metastatic melanoma at liver.

ACKNOWLEDGEMENTS

This work was supported by grants from the West Bengal Department of Science and Technology and Biotechnology [Grant sanctioned memo no: 551 (Sanc.)/ ST/P/S&T/9G-20/2014, dated 18.03.2014]. Authors are thankful to Dr. Indraneel Saha from Sarsuna College, Kolkata for helping in ectopic animal model development, Mr. Mriganka Biswas from Chota Jagulia High School (H.S), Chhota Jagulia, North 24 Parganas, West Bengal, Dr. Sajal Dey from Sripat Singh College, Jiaganj, West Bengal for critical comment, scientific discussion and helpful suggestions and Dr. Anway Sen from Nil Ratan Sircar Medical College and Hospital, Kolkata for Biopsy and tissue identification.

Declaration of competing interest: The authors declare that there are no conflicts of interests.

Author Contribution: SC and DP performed the experiments, maintained cell line, developed experimental mice model, contributed in research designing, assisted in data analysis and manuscript preparation. PG and SB helped in sample preparation, enzyme analysis, protein quantification and also involved in manuscript preparation. KDC participated in research idea development, contributed in experimental designing and execution, data analysis and manuscript preparation. PC participated in data representation and manuscript preparation. AB and GCS participated in research idea development, experiment designing, data analysis and editing of manuscript.

REFERENCES

Bostanci, O., Kartal, K. and Battal, M., (2014). Liver metastases of unknown primary: Malignant melanoma. Case Reports in Hepatology, 2014.

Böckmann, S. and Hinz, B., (2020). Cannabidiol Promotes Endothelial Cell Survival by Heme Oxygenase-1-Mediated Autophagy. Cells, 9(7), p.1703.

Capaci, V., Bascetta, L., Fantuz, M., Beznoussenko, G.V., Sommaggio, R., Cancila, V., Bisso, A., Campaner, E., Mironov, A.A., Wisniewski, J.R. and Severino, L.U., (2020). Mutant p53 induces Golgi tubulo-vesiculation driving a prometastatic secretome. Nature communications, 11(1), pp.1-19.

Chan, Z.C.K., Oentaryo, M.J. and Lee, C.W., (2020). MMP-mediated modulation of ECM environment during axonal growth and NMJ development. Neuroscience Letters, 724, p.134822.

Chao, X., Wang, G., Tang, Y., Dong, C., Li, H., Wang, B., Wu, J. and Zhao, J., (2019). The effects and mechanism of peiminine-induced apoptosis in human hepatocellular carcinoma HepG2 cells. Plos one, 14(1), p.e0201864.

Chatterjee, S., Patra, D., Chakraborti, U., Sengupta, D., Ghosh, P., Basu, A., Sadhukhan, G.C. and Chowdhury, K.D., (2019). Association of p38MAPK-p53-Fas aggregation in S-allyl cysteine mediated regulation of hepatocarcinoma. Environmental toxicology, 34(8), pp.928-940.

Chen, X.M., Zhang, M., Fan, P.L., Qin, Y.H. and Zhao, H.W., (2016). Chelerythrine chloride induces apoptosis in renal cancer HEK-293 and SW-839 cell lines. Oncology letters, 11(6), pp.3917-3924.

Chowdhury, K.D., Sarkar, A., Chatterjee, S., Patra, D., Sengupta, D., Banerjee, S., Chakraborty, P. and Sadhukhan, G.C., (2019). Cathepsin B mediated scramblase activation triggers cytotoxicity and cell cycle arrest by andrographolide to overcome cellular resistance in cisplatin resistant human hepatocellular carcinoma HepG2 cells. Environmental toxicology and pharmacology, 68, pp.120-132.

Chmura, S.J., Dolan, M.E., Cha, A., Mauceri, H.J., Kufe, D.W. and Weichselbaum, R.R., (2000). In vitro and *in vivo* activity of protein kinase C inhibitor chelerythrine chloride induces tumor cell toxicity and growth delay *in vivo*. Clinical Cancer Research, 6(2), pp.737-742.

Connor, A.A., Denroche, R.E., Jang, G.H., Lemire, M., Zhang, A., Chan-Seng-Yue, M., Wilson, G., Grant, R.C., Merico, D., Lungu, I. and Bartlett, J.M., (2019). Integration of genomic and transcriptional features in pancreatic cancer reveals increased cell cycle progression in metastases. Cancer Cell, 35(2), pp.267-282.

Dahal, P., Guerin, P.J., Price, R.N., Simpson, J.A. and Stepniewska, K., (2019). Evaluating antimalarial efficacy in single-armed and comparative drug trials using competing risk survival analysis: a simulation study. BMC medical research methodology, 19(1), p.107.

Eggermont, A.M., Kicinski, M., Blank, C.U., Mandala, M., Long, G.V., Atkinson, V., Dalle, S., Haydon, A., Khattak, A., Carlino, M.S. and Sandhu, S., (2020). Association between immune-related adverse events and recurrence-free survival among patients with stage III melanoma randomized to receive pembrolizumab or placebo: a secondary analysis of a randomized clinical trial. JAMA oncology, 6(4), pp.519-527.

Enninga, E.A.L., Moser, J.C., Weaver, A.L., Markovic, S.N., Brewer, J.D., Leontovich, A.A., Hieken, T.J., Shuster, L., Kottschade, L.A., Olariu, A. and Mansfield, A.S., (2017). Survival of cutaneous melanoma based on sex, age, and stage in the United States, 1992–2011. Cancer medicine, 6(10), pp.2203-2212.

Fares, J., Fares, M.Y., Khachfe, H.H., Salhab, H.A. and Fares, Y., (2020). Molecular principles of metastasis: a hallmark of cancer revisited. Signal transduction and targeted therapy, 5(1), pp.1-17.

Galli, A., Svegliati-Baroni, G., Ceni, E., Milani, S., Ridolfi, F., Salzano, R., Tarocchi, M., Grappone, C., Pellegrini, G., Benedetti, A. and Surrenti, C., (2005). Oxidative stress stimulates proliferation and invasiveness of hepatic stellate cells via a MMP2-mediated mechanism. Hepatology, 41(5), pp.1074-1084.

Hakimzadeh, H., Ghazanfari, T., Rahmati, B. and Naderimanesh, H., (2010). Cytotoxic effect of garlic extract and its fractions on Sk-mel3 melanoma cell line. Immunopharmacology and immunotoxicology, 32(3), pp.371-375.

He, N., Wang, P., Wang, P., Ma, C. and Kang, W., (2018). Antibacterial mechanism of chelerythrine isolated from root of *Toddalia asiatica* (Linn) Lam. BMC complementary and alternative medicine, 18(1), p.261.

He, H., Zhuo, R., Dai, J., Wang, X., Huang, X., Wang, H. and Xu, D., (2020). Chelerythrine induces apoptosis via ROS-mediated endoplasmic reticulum stress and STAT3 pathways in human renal cell carcinoma. Journal of Cellular and Molecular Medicine, 24(1), pp.50-60.

Hao, Y., Baker, D. and ten Dijke, P., (2019). TGF-β-mediated epithelial-mesenchymal transition and cancer metastasis. International journal of molecular sciences, 20(11), p.2767.

Jones, O.T., Ranmuthu, C.K., Hall, P.N., Funston, G. and Walter, F.M., (2020). Recognising Skin Cancer in Primary Care. Advances in Therapy, 37(1), pp.603-616.

Kapinova, A., Kubatka, P., Liskova, A., Baranenko, D., Kruzliak, P., Matta, M., Büsselberg, D., Malicherova, B., Zulli, A., Kwon, T.K. and Jezkova, E., (2019). Controlling metastatic cancer: the role of phytochemicals in cell signaling. Journal of Cancer Research and Clinical Oncology, 145(5), pp.1087-1109.

Kanamori, Y., Dalla Via, L., Macone, A., Canettieri, G., Greco, A., Toninello, A. and Agostinelli, E., (2020). Aged garlic extract and its constituent, S allyl L cysteine, induce the apoptosis of neuroblastoma cancer cells due to mitochondrial membrane depolarization. Experimental and Therapeutic Medicine, 19(2), pp.1511-1521.

Kemény-Beke, Á., Aradi, J., Damjanovich, J., Beck, Z., Facskó, A., Berta, A. and Bodnár, A., (2006). Apoptotic response of uveal melanoma cells upon treatment with chelidonine, sanguinarine and chelerythrine. Cancer letters, 237(1), pp.67-75.

Kumar, S., Deepak, P., Gautam, P.K. and Acharya, A., (2013). A benzophenanthridine alkaloid, chelerythrine induces apoptosis *in vitro* in a Dalton's lymphoma. Journal of cancer research and therapeutics, 9(4), p.693.

Kumar, S., Tomar, M.S. and Acharya, A., (2015). Chelerythrine delayed tumor growth and increased survival duration of Dalton's lymphoma bearing BALB/c H 2d mice by activation of NK cells *in vivo*. Journal of Cancer Research and Therapeutics, 11(4), p.904.

Lala, V., Goyal, A., Bansal, P. and Minter, D., (2020). Liver function tests. StatPearls.

Li, Y. and Martin, R.C., (2011). Herbal medicine and hepatocellular carcinoma: applications and challenges. Evidence-Based Complementary and Alternative Medicine, 2011.

Li, X., Qian, X., Jiang, H., Xia, Y., Zheng, Y., Li, J., Huang, B.J., Fang, J., Qian, C.N., Jiang, T. and Zeng, Y.X., (2018). Nuclear PGK1 alleviates ADP-dependent inhibition of CDC7 to promote DNA replication. Molecular cell, 72(4), pp.650-660.

Li, Z., Guo, D., Yin, X., Ding, S., Shen, M., Zhang, R., Wang, Y. and Xu, R., (2020). Zinc oxide nanoparticles induce human multiple myeloma cell death via reactive oxygen species and Cyt-C/Apaf-1/Caspase-9/Caspase-3 signaling pathway *in vitro*. Biomedicine & Pharmacotherapy, 122, p.109712.

lin Lin, X., Li, K., Yang, Z., Chen, B. and Zhang, T., (2020). Dulcitol suppresses proliferation and migration of hepatocellular carcinoma via regulating SIRT1/p53 pathway. Phytomedicine, 66, p.153112.

Ng, K.T., Guo, D.Y., Cheng, Q., Geng, W., Ling, C.C., Li, C.X., Liu, X.B., Ma, Y.Y., Lo, C.M., Poon, R.T. and Fan, S.T., (2012). A garlic derivative, S-allylcysteine (SAC), suppresses proliferation and metastasis of hepatocellular carcinoma. PLoS One, 7(2), p.e31655.

Palmer, T.D., Ashby, W.J., Lewis, J.D. and Zijlstra, A., (2011). Targeting tumor cell motility to prevent metastasis. Advanced drug delivery reviews, 63(8), pp.568-581.

Phillips, D.C., Jin, S., Gregory, G.P., Zhang, Q., Xue, J., Zhao, X., Chen, J., Tong, Y., Zhang, H., Smith, M. and Tahir, S.K., (2020). A novel CDK9 inhibitor increases the efficacy of venetoclax (ABT-199) in multiple models of hematologic malignancies. Leukemia, 34(6), pp.1646-1657.

Reiners Jr, J.J., Caruso, J.A., Mathieu, P., Chelladurai, B., Yin, X.M. and Kessel, D., (2002). Release of cytochrome c and activation of pro-caspase-9 following lysosomal photodamage involves Bid cleavage. Cell Death & Differentiation, 9(9), pp.934-944.

Ruini, C., Haas, C., Mastnik, S., Knott, M., French, L.E., Schlaak, M. and Berking, C., (2020). Primary Biliary Cirrhosis and Granulomatous Hepatitis After Immune Checkpoint Blockade in Patients with Metastatic Melanoma: Report of 2 Cases and Literature Discussion. Journal of Immunotherapy (Hagerstown, Md.: 1997).

Sandru, A., Voinea, S., Panaitescu, E. and Blidaru, A., (2014). Survival rates of patients with metastatic malignant melanoma. Journal of medicine and life, 7(4), p.572.

Sang, S., Li, S., Fan, W., Wang, N., Gao, M. and Wang, Z., (2019). Zinc thiazole enhances defense enzyme activities and increases pathogen resistance to *Ralstonia solanacearum* in peanut (Arachis hypogaea) under salt stress. Plos one, 14(12), p.e0226951.

Schirrmacher, V., (2019). From chemotherapy to biological therapy: A review of novel concepts to

reduce the side effects of systemic cancer treatment. International journal of oncology, 54(2), pp.407-419.

Sengupta, D., Chatterjee, S., Chatterjee, T., Chowdhury, K.D., Bhowmick, P., Chakraborti, U., Sarkar, A., Paul, S., Sur, P.K. and Sadhukhan, G.C., A, June (2017). SAC and Berberine mediated repression of reactive species and hepatoprotection after DEN+ CCl 4 exposure. In Proceedings of the Zoological Society (Vol. 70, No. 1, pp. 28-41). Springer India.

Sengupta, D., Chowdhury, K.D., Chatterjee, S., Sarkar, A., Paul, S., Sur, P.K. and Sadhukhan, G.C., (2017 B). Modulation of adenylate cyclase signaling in association with MKK3/6 stabilization under combination of SAC and berberine to reduce HepG2 cell survivability. Apoptosis, 22(11), pp.1362-1379.

Sengupta, D., Chowdhury, K.D., Sarkar, A., Paul, S. and Sadhukhan, G.C., (2014). Berberine and S allyl cysteine mediated amelioration of DEN+ CCl4 induced hepatocarcinoma. Biochimica et Biophysica Acta (BBA)-General Subjects, 1840(1), pp.219-244.

Shang, A., Cao, S.Y., Xu, X.Y., Gan, R.Y., Tang, G.Y., Corke, H., Mavumengwana, V. and Li, H.B., (2019). Bioactive compounds and biological functions of garlic (*Allium sativum* L.). Foods, 8(7), p.246.

Simoes Eugénio, M., Farooq, M., Dion, S., Devisme, C., Raguenes-Nicol, C., Piquet-Pellorce, C., Samson, M., Dimanche-Boitrel, M.T. and Le Seyec, J., (2020). Hepatocellular Carcinoma Emergence in Diabetic Mice with Non-Alcoholic Steatohepatitis Depends on Diet and Is Delayed in Liver Exhibiting an Active Immune Response. Cancers, 12(6), p.1491.

Somade, O.T., Ajayi, B.O., Olunaike, O.E. and Jimoh, L.A., (2020). Hepatic oxidative stress, up-regulation of pro-inflammatory cytokines, apoptotic and oncogenic markers following 2-methoxyethanol administrations in rats. Biochemistry and biophysics reports, 24, p.100806.

Sundararajan, S., Thida, A.M. and Badri, T., (2020). Metastatic Melanoma. StatPearls [Internet].

Tan, L., Sandhu, S., Lee, R.J., Li, J., Callahan, J., Ftouni, S., Dhomen, N., Middlehurst, P., Wallace, A., Raleigh, J. and Hatzimihalis, A., (2019). Prediction and monitoring of relapse in stage III melanoma using circulating tumor DNA. Annals of Oncology, 30(5), pp.804-814.

Teijido, O. and Dejean, L., (2010). Upregulation of Bcl2 inhibits apoptosis-driven BAX insertion but favors BAX relocalization in mitochondria. FEBS letters, 584(15), pp.3305-3310.

Viswanadha, V.P., Dhivya, V., Beeraka, N.M., Huang, C.Y., Gavryushova, L.V., Minyaeva, N.N., Chubarev, V.N., Mikhaleva, L.M., Tarasov, V.V. and Aliev, G., (2020). The protective effect of piperine against isoproterenol-induced inflammation in experimental models of myocardial toxicity. European Journal of Pharmacology, 885, p.173524.

Wang, H., Oo Khor, T., Shu, L., Su, Z.Y., Fuentes, F., Lee, J.H. and Tony Kong, A.N., (2012). Plants vs. cancer: a review on natural phytochemicals in preventing and treating cancers and their druggability. Anti-Cancer Agents in Medicinal Chemistry (Formerly Current Medicinal Chemistry-Anti-Cancer Agents), 12(10), pp.1281-1305.

Wu, S., Yang, Y., Li, F., Huang, L., Han, Z., Wang, G., Yu, H. and Li, H., (2018). Chelerythrine induced cell death through ROS-dependent ER stress in human prostate cancer cells. OncoTargets and therapy, 11, p.2593.

Xu, Y.S., Feng, J.G., Zhang, D., Zhang, B., Luo, M., Su, D. and Lin, N.M., (2014). S-allylcysteine, a garlic derivative, suppresses proliferation and induces apoptosis in human ovarian cancer cells *in vitro*. Acta Pharmacologica Sinica, 35(2), pp.267-274.

Yang, B., Zhang, D., Qian, J. and Cheng, Y., (2020). Chelerythrine suppresses proliferation and metastasis of human prostate cancer cells via modulating MMP/TIMP/NF-κB system. Molecular and Cellular Biochemistry, 474(1), pp.199-208.

Yau, W.W., Singh, B.K., Lesmana, R., Zhou, J., Sinha, R.A., Wong, K.A., Wu, Y., Bay, B.H., Sugii, S., Sun, L. and Yen, P.M., (2019). Thyroid hormone (T3) stimulates brown adipose tissue activation via mitochondrial biogenesis and MTOR-mediated mitophagy. Autophagy, 15(1), pp.131-150.

Zbytek, B., Carlson, J.A., Granese, J., Ross, J., Mihm, M. and Slominski, A., (2008). Current concepts of metastasis in melanoma. Expert review of dermatology, 3(5), pp.569-585.

Zhou, Y., Yan, H., Guo, M., Zhu, J., Xiao, Q. and Zhang, L., (2013). Reactive oxygen species in vascular formation and development. Oxidative medicine and cellular longevity, 2013.